Supplementary material

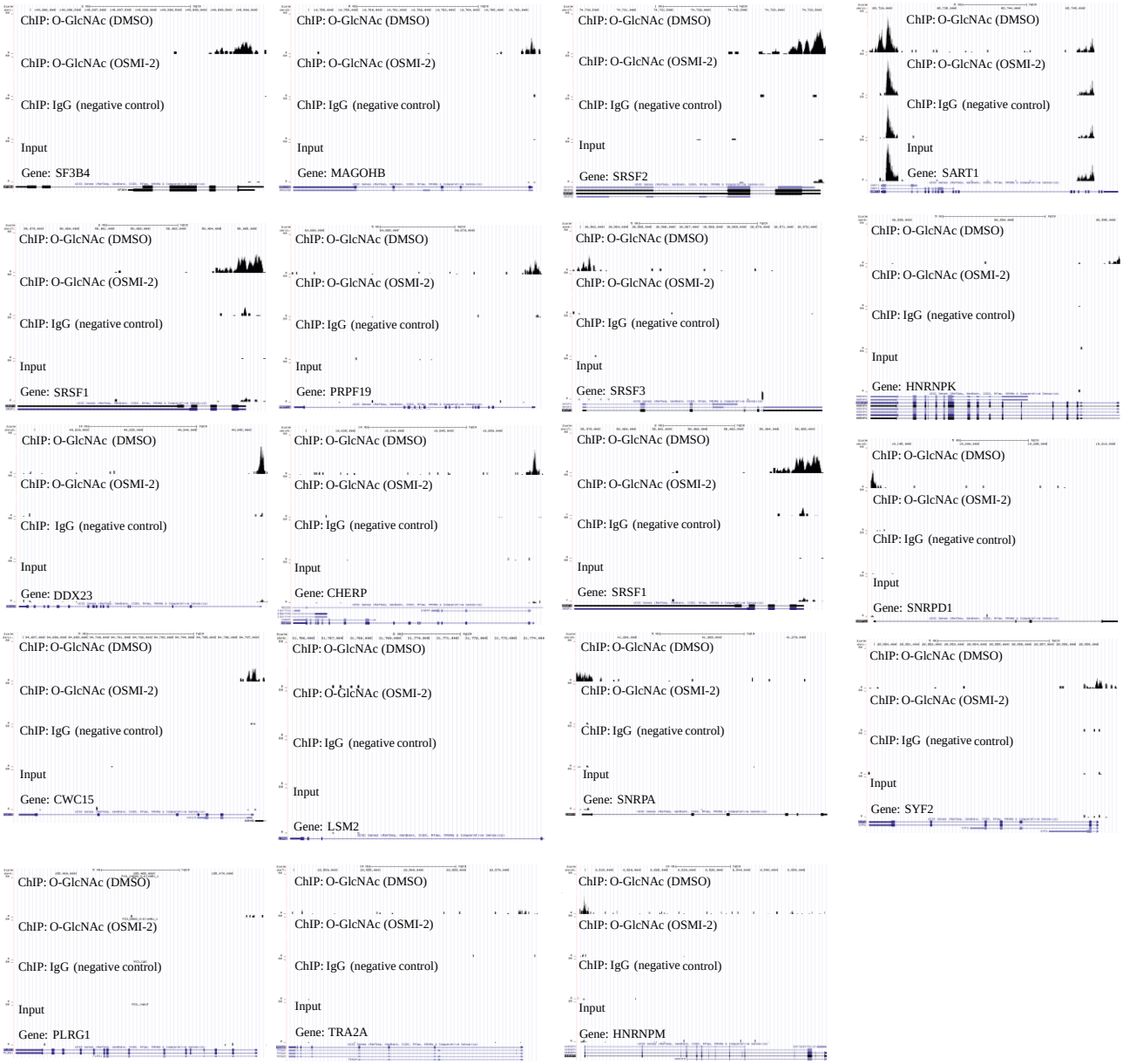

Supplementary Figure 1. Chromatin O-GlcNAc on the promoters of the spliceosome genes is removed when cells are treated with the OGT inhibitor. The figure depicts O-GlcNAc enrichment on the promoters of the mRNAs that constitute the spliceosome mRNAs based on pathway enrichment presented in the main figure 1 B. These mRNAs were identified to be increased in response to 0.5µM AT7519 treatment but not increased when 0.5µM AT7519 was combined with OGT inhibitor 40µM OSMI-2 or OGT knockdown. The figure shows .wig-files generated from a previously published chromatin immunoprecipitation coupled to massively parallel sequencing data (GSE121474).

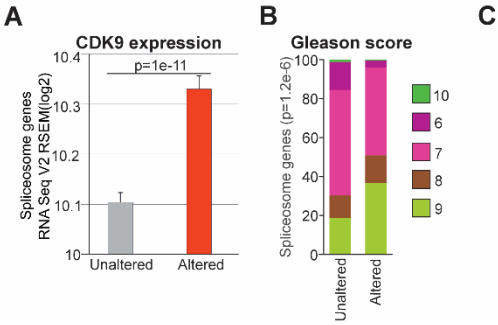

C

Clinical Attribute	Statistical Test	p-Value	q-Value
Fraction Genome Altered	Kruskal Wallis Test	< 10-10	5,56E-09
Gleason pattern primary	Kruskal Wallis Test	3,15E-07	1,04E-05
Radical Prostatectomy Gleason Score for Prostate Cancer	Chi-squared Test	1,08E-06	2,38E-05
American Joint Committee on Cancer Tumor Stage Code	Chi-squared Test	6,73E-04	0,0106
Disease Free Status	Chi-squared Test	8,04E-04	0,0106
Mutation Count	Kruskal Wallis Test	1,01E-03	0,0111
Ct scan ab pelvis indicator	Chi-squared Test	2,66E-03	0,0251
Form completion date	Chi-squared Test	3,48E-03	0,0287
Person Neoplasm Status	Chi-squared Test	4,78E-03	0,0351
Gleason pattern secondary	Kruskal Wallis Test	7,27E-03	0,0421
Biochemical Recurrence Indicator	Chi-squared Test	7,41E-03	0,0421
Positive Finding Lymph Node Hematoxylin and Eosin Staining Microscopy Count	Kruskal Wallis Test	7,65E-03	0,0421

Supplementary Figure 2. Alterations in the spliceosome-component mRNAs identify aggressive prostate cancer cases that overexpress CDK9. A) Alterations in spliceosomal mRNAs induced by CDK9-inhibition in an OGT-dependent manner are found in 50% of prostate cancer patients and this patient group shows increased expression of CDK9 (relates to main figure 1B). Data was generated using the cBioPortal and the changes in the spliceosome mRNAs (up-/downregulation and deletion/amplification) were assessed in the TCGA dataset. **B and C)** Alterations in spliceosomal mRNAs induced by CDK9-inhibition in an OGT-dependent manner identify aggressive prostate cancers.

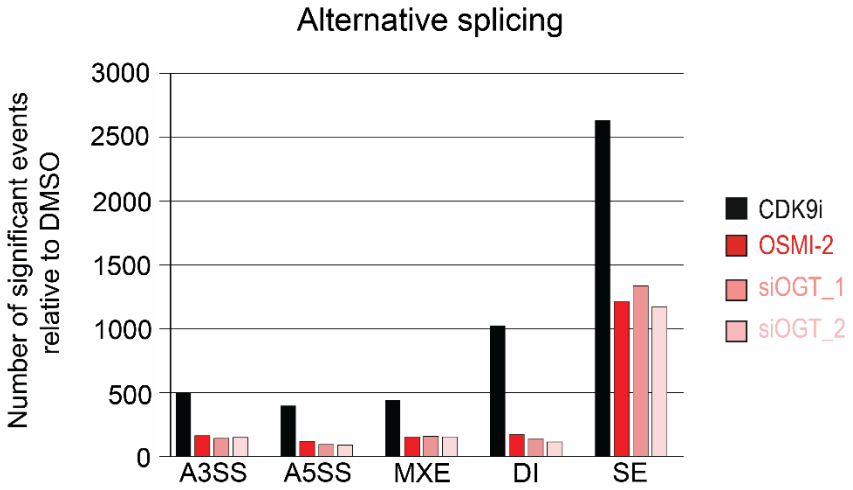

Supplementary Figure 3. Number of significant alternative splicing events. The rMATS v4.1.0 *(1)* was used to determine the differential alternative splicing events between different conditions. The bioconductor package Rcwl was used to perform reproducible analysis through the Common Workflow Language (CWL). Five types of alternative splicing events based on the GENCODE gene annotation were evaluated (alternative 3′ splice site; A3SS, alternative 5′ splice site; A5SS, mutually exclusive exons; MXE, detained intron; DI and skipped exon; SE. The events with inclusion-level difference $\geq 10\%$, and FDR < 0.1 were determined as differential alternative splicing events.

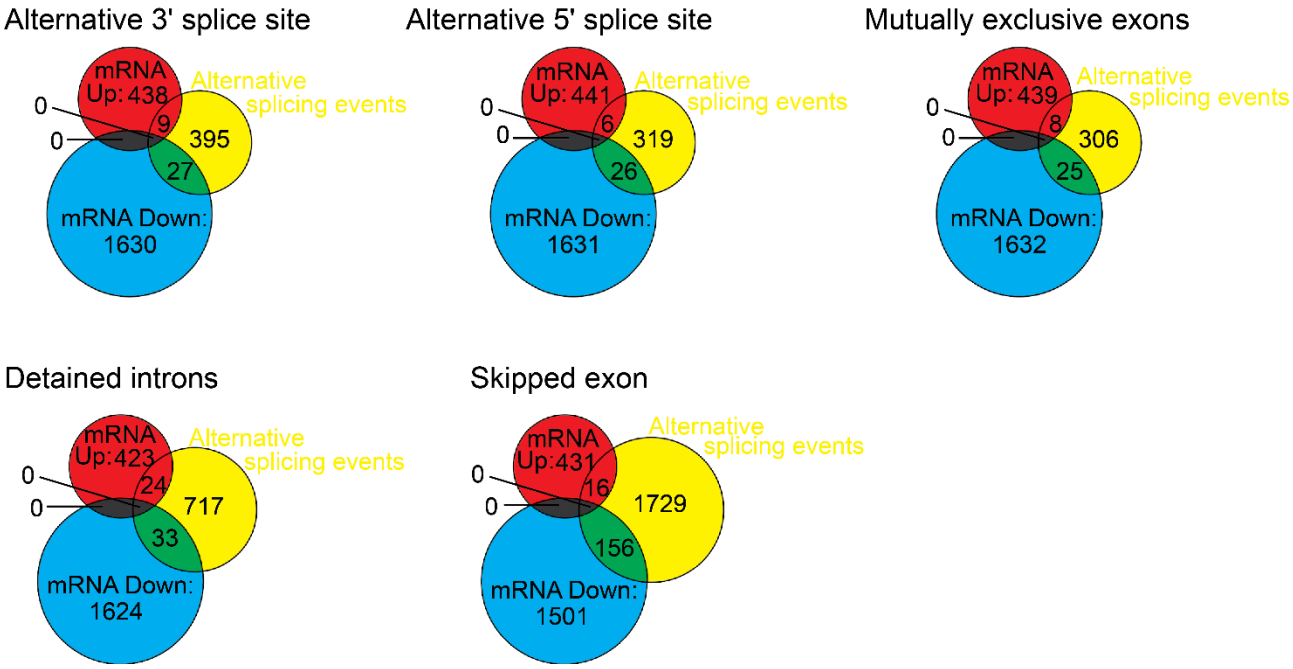

Supplementary Figure 4. Correlation between mRNA levels and alternative splicing events. RNA-seq data was used to generate lists of differentially expressed genes in response to AT7519 treatment (log2(FC)±>1, p<0.01) that were overlapped with the alterative splicing data.

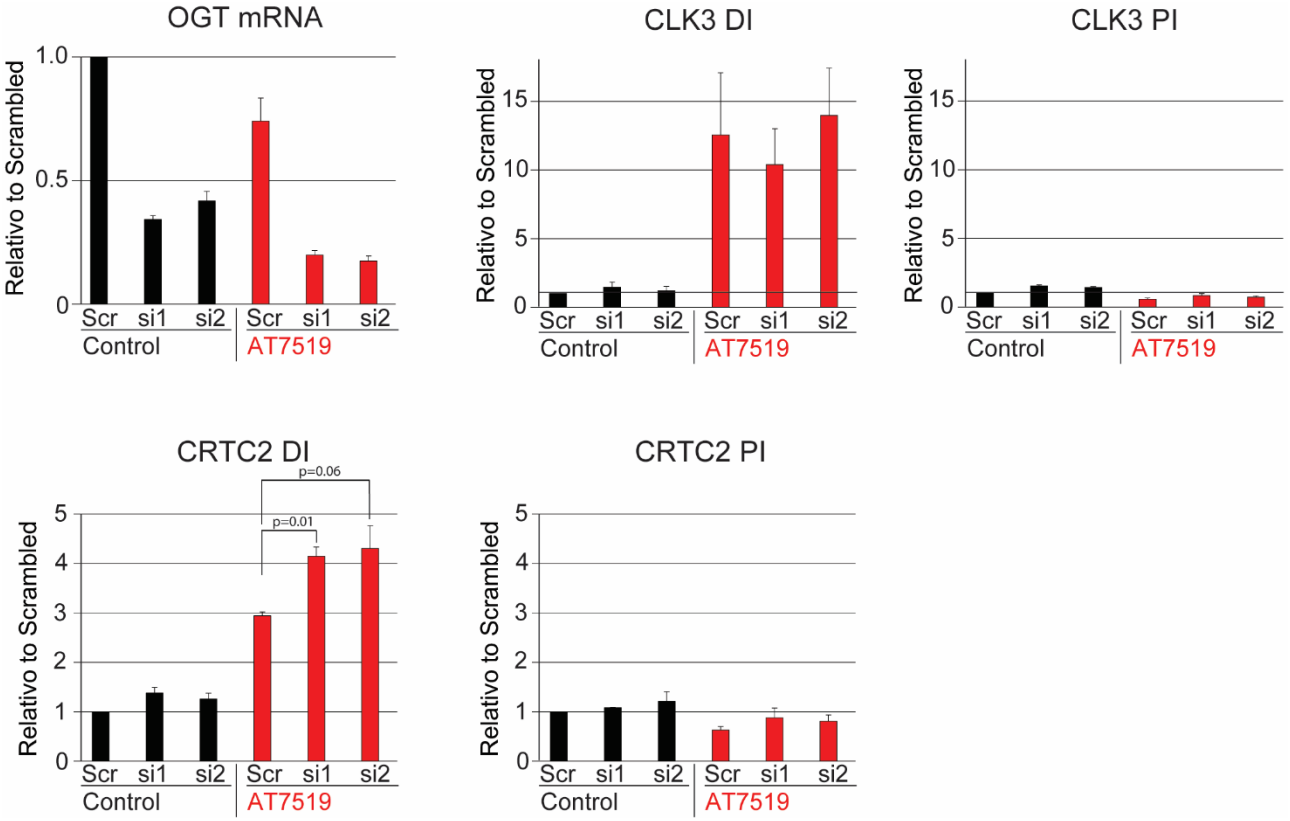

Supplementary Figure 5. Effects of OGT knockdown on CDK9-inhibitor induced alternative splicing. OGT knockdown (si1 and si2) was performed for 48 hours and cells were treated with either DMSO (control) or 0.5µM AT7519 (CDK9 inhibitor) for the last 4 hours. mRNA was isolated and used for RT-qPCR. Data shown is an average of 3-4 biological replicates and Student's t-test was used to assess the statistical significance.

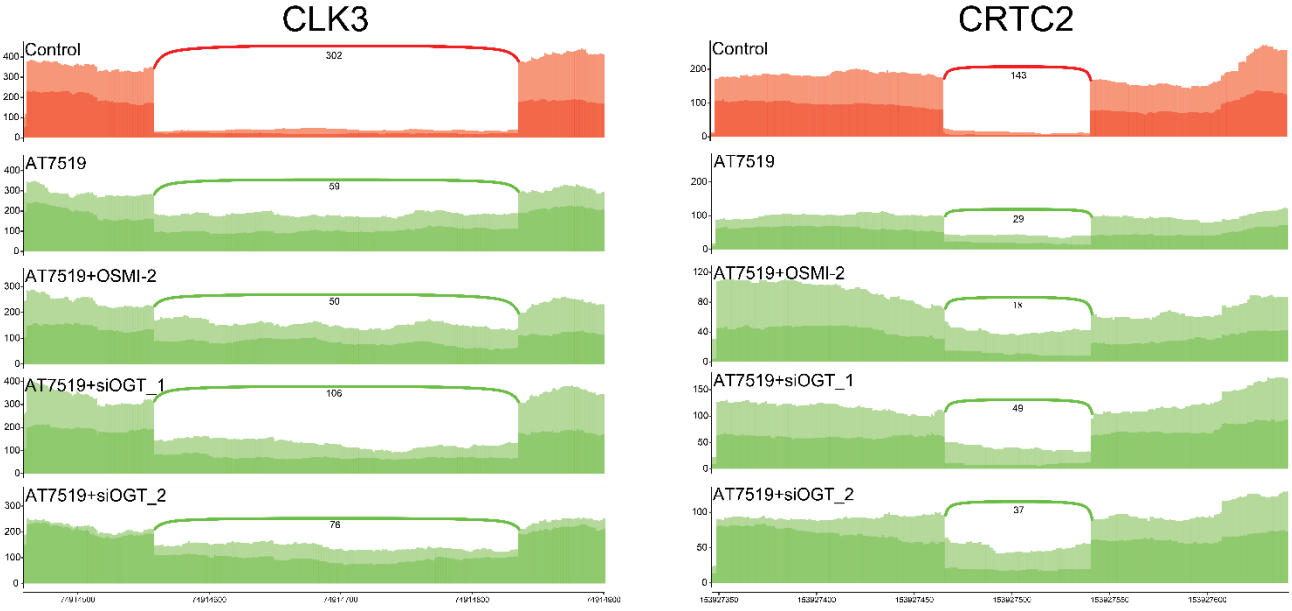

Supplementary Figure 6. The effect of CDK9 inhibitor and co-targeting of CDK9 and OGT on intron detention of CLK3 and CRTC2 mRNAs. OGT knockdown was performed for 48 hours and cells were treated with either DMSO (control) or 0.5µM AT7519 (CDK9 inhibitor) or 40µM OSMI-2 for the last 4 hours. Samples were analyzed using RNA-seq. The histograms show poly(A) reads for the samples. The Y-axis is the number of reads normalized to read density, and the number of junction spanning reads for detained intron are also shown.

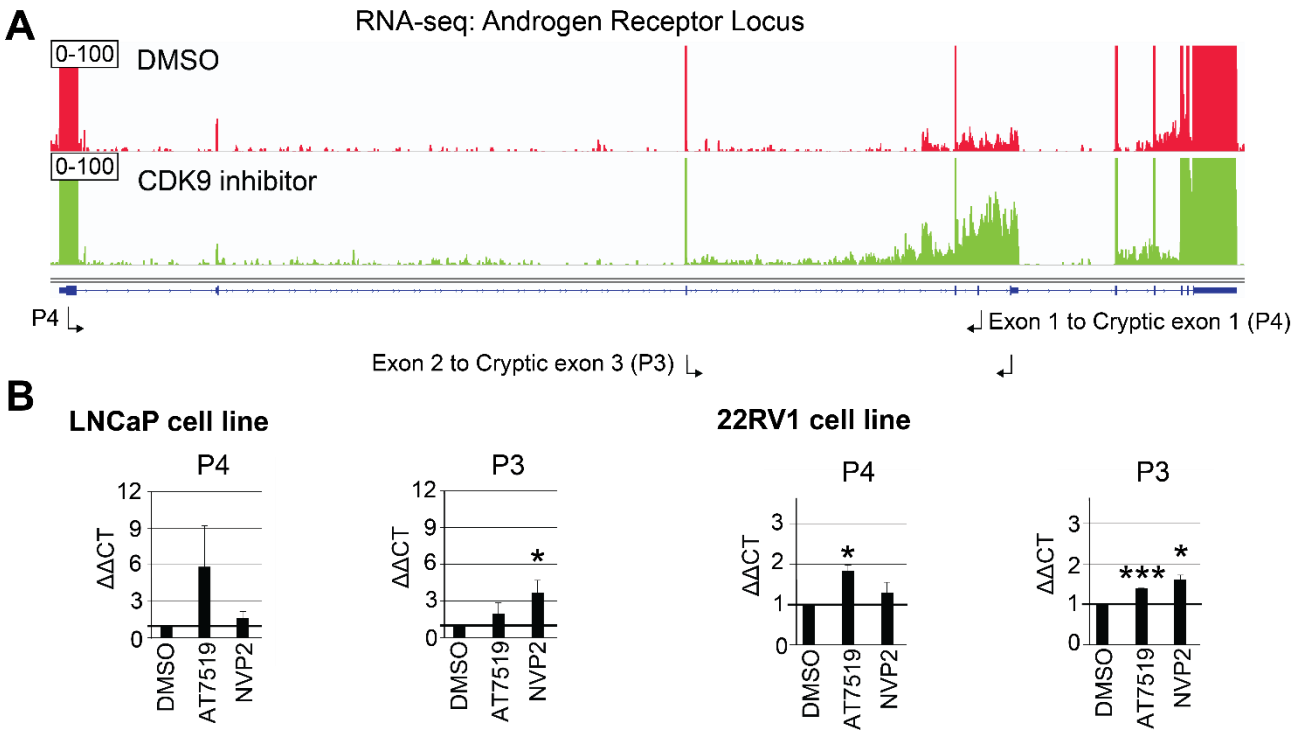

Supplementary Figure 7. The effect of CDK9 inhibitor on AR mRNA. Integrative genomics viewer was used to visualize RNA-seq data for the AR locus (note that this is the same figure as in the main figure 3A; it is used here to illustrate the positions of the primer pairs used). Cells were treated as indicated for 4 hours and analyzed using RT-qPCR. The primers used are indicated in Supplementary figure 7A below the AR gene using small arrows: these primers were selected from an earlier publication [(2)]. Data shown are average of 4 biological replicates with SEM; Student's t test was used to assess the statistical significance; *, $P < 0.05$ and *** $P < 0.001$.

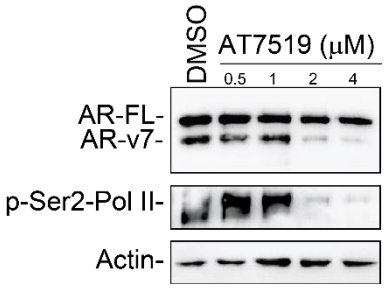

Supplementary Figure 8. The effect of AT7519 on the androgen receptor protein in 22RV1 cells. Cells were treated for 24 hours and proteins of interest were detected using western blot. Data shown is representative of two biological replicates.

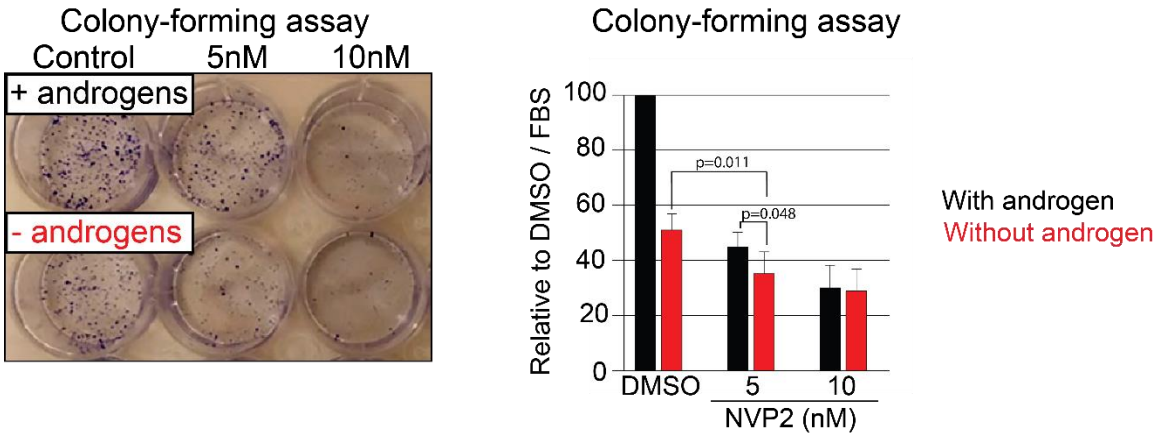

Supplementary Figure 9. Inhibition of CDK9 decreases proliferation of castration resistant prostate cancer (CRPC) cells. Colony formation assay of 22RV1 cells treated with NVP2 in the presence and absence of androgens. Data shown are average of four biological replicates with SEM; Student's t test was used to assess the statistical significance. All of the treatments were normalized to cells grown in the presence of androgens and treated with the vehicle (DMSO). Note that in these experiments values were not normalized to the background, which gives higher overall signal.

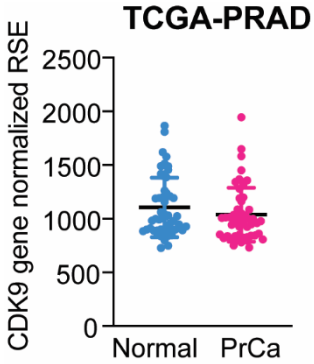

Supplementary Figure 10. Expression of CDK9 is not affected in primary prostate cancer. The Cancer Genome Atlas data for prostate adenocarcinoma was used to evaluate the expression of CDK9 in the primary prostate cancer.

Supplementary Table 5. Primers used in this study.

Name	Forward	Reverse	This publication or reported earlier (PMID)
Normal AR	AAGACCTGCCTGATCTGTGG	CGAAGACGACAAGATGGACA	This publication
A3SS	AAGACCTGCCTGATCTGTGG	TGGACAGAGTATGGCACCAA	This publication
P4	GTTGCTCCCGCAAGTTTCCTTCTC	CTGTTGTGGATGAGCAGCTGAGAGTCT	PMID: 19117982
P3	TGTCACTATGGAGCTCTCACATGTGG	CTGTGGATCAGCTACTACCTTCAGCTC	PMID: 19117982
Actin	TGGGACGACATGGAGAAAAT	AGAGGCGTACAGGGATAGCA	This publication
OGT PI	ACTGTGTTCGCAGTGACCTG	CAAATTTCCCCTTGTGCATT	This publication
OGT DI	ACTGTGTTCGCAGTGACCTG	AGTTGAAGACTTGGCAAAAAGT	This publication
CLK3 PI	TTCACGTTCTCGTCATCGTC	CAGGTGACCCTCCTTGTCAT	This publication
CLK3 DI	TTCACGTTCTCGTCATCGTC	AGCCAGCACACTCTGGCTAC	This publication
CRTC2 PI	ACTGGCATACACAAGGAGCT	GGACACCATTCTTCGAGGATC	This publication
CRTC2 DI	ACTGGCATACACAAGGAGCT	AGAAGTCAGCAGAGGAAGCA	This publication

References:

1. Shen, S., Park, J.W., Lu, Z.X., Lin, L., Henry, M.D., Wu, Y.N., Zhou, Q. and Xing, Y. (2014) rMATS: robust and flexible detection of differential alternative splicing from replicate RNA-Seq data. *Proc Natl Acad Sci U S A*, **111**, E5593-5601.
2. Hu, R., Dunn, T.A., Wei, S., Isharwal, S., Veltri, R.W., Humphreys, E., Han, M., Partin, A.W., Vessella, R.L., Isaacs, W.B. *et al.* (2009) Ligand-independent androgen receptor variants derived from splicing of cryptic exons signify hormone-refractory prostate cancer. *Cancer Res*, **69**, 16-22.